levels of ambient noise spectrum are assumed, namely calm, moderate, and severe. These assumptions reflect the wind-generated noise and associate them to the sea states scale as depicted in Wenz curve [12]. A "calm" assumption is associated to the sea state of 0.5. In this state, the noise is created by a calm sea with waves reaching up to 0.1 meter in average. A "moderate" level is referred to as the noise induced by the sea with sea state of 4. At this level, the waves may reach a height of 3 meter in average. The highest noise level is attained when the sea is in "severe" state, which is caused by the wind that brings the sea waves up to 7 meters height. This state represents a sea scale of 6 in Wenz curve. In our case study, the underwater sensor transmits pressure data with some attributes, including the date, time, and battery status. We consider a 120 bit frame length to be sufficient to accommodate these data, including the frame overhead. We also assume that no forward error correction scheme is applied.

To deal with different ambient noise levels, this paper defines three design parameters, namely the link reliability constraint, acoustic carrier frequency and underwater transmission rate. This paper derives the optimal configuration and the implementation cost with these design parameters varied and analyze the results under different ambient noise conditions.

B. Cost Function Assumption

To limit the scope of analysis, the case study only focuses on linear cost function. Our discussion associates the variable Q to two independent quantities. They mainly represent the physical attributes with respect to the infrastructure's component. More specifically, the fiber optic implementation cost is governed by the length of fiber optic L and the fiber optic transmission rate r_f, whereas the underwater sensor network cost is dictated by the number of nodes N_h and the node's transmission rate r_s. The following two equations express the cost function for the fiber optic and the undersea sensor network, respectively.

$$C_F = \phi_f \cdot r_f \cdot L$$
$$C_S = \phi_s \cdot r_s \cdot N_h \tag{15}$$

To carry the cost analysis, the unit cost of sensor ϕ_s is normalized to the fiber optic unit cost ϕ_f such that $\phi_s = \gamma\phi_f$. The total cost,C_{tot}, is expressed as the ratio of the cost of the most expensive solution. Without loss of generality, we assume that the initial deployment cost of the fiber optic and undersea sensors are the same.

C. Formulation for Data Delivery Time

Both the fiber optic and multi-hop acoustic links use automatic repeat request (ARQ) as the retransmission scheme. A stop and wait ARQ will be implemented in a per-hop basis. Consequently, the round trip transmission time of a packet and its associated acknowledgment can be expressed as follows:

$$t_{rt}(d) = t_m + 2t_p(d) + t_a$$

The parameter t_m represents the data transmission time, $t_p(d)$ the acoustic propagation time traversing through a link of length d and t_a the acknowledgment packet transmission time. Given the reliability function, $R(\Delta, \boldsymbol{d})$, the average delay

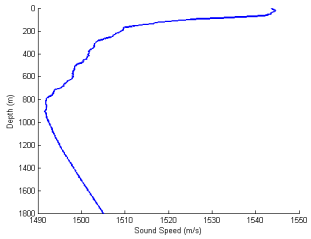

Fig. 6: Courtesy of BPPT [15]: Underwater Sound Speed around of our case study area

to transmit a packet and receive its acknowledgment can be expressed as follows:

$$\mathcal{T} = \frac{1}{R(\Delta, \boldsymbol{d})} \cdot t_{rt}(d) \tag{16}$$

Eq. (16) is applicable for both fiber optic and acoustic links. Based on Eq. (7), we can deduce a formulation for total data delivery time, $\tau_{net}()$, as follows :

$$\tau_{net}(\Delta, \boldsymbol{d}) = \frac{t^F_{rt}(L)}{R^F(\Delta, \boldsymbol{d})} + \sum_{i=1}^{N_h} \frac{t^S_{rt}(d^i)}{R^i(\Delta, \boldsymbol{d})} \tag{17}$$

In the above equation, t^F_{rt} denotes the round trip time transmission in the fiber optic link and $t^S_{rt}(d^i)$ is the round trip time transmission in acoustic link i. In the proposed heuristic, Eq. (17) is invoked each time the timeliness constraint is verified with a new value of N_h being assigned for each invocation. In this paper, the fiber optic reliability is considered hight, i.e. $R^F \approx 1$. Thus, the data delivery time in fiber optic link, $\mathcal{T}^F$ is approximately equal to t^F_{rt}.

D. Assumption on Bit Error Probability Distribution Function

The case study uses binary frequency shift keying (BFSK) for the modulation scheme. To calculate bit error probability, this paper adopts the probability distribution function formulated in [16]. Let $\frac{E^i_b}{N^i_0}$ be the ratio of bit energy to equivalent white noise at link i. The bit error probability at link i can be expressed as follows:

$$BER^i_r(\Delta, \boldsymbol{d}) = \frac{v}{\Gamma(v)} \int_0^\infty u^{v-1} \left(2v + u\frac{E^i_b}{N^i_0}\right) du \tag{18}$$

In the above equation, $\Gamma()$ represents the Gamma function, with $u = y^2$, where y is the real part of complex value of signal amplitude random variable.

E. Underwater Sound Speed and Sea Floor profile

Figure 6 shows the characteristic of the underwater sound speed associated with the area under study. The figure shows that the speed of the acoustic wave drops rapidly in shallow waters of around 100 to 200 meters. The decrease in speed in deeper waters continue but at lower rate and re-bounce at a depth of about 800 meters. This profile is obtained by applying the measurement data collected by [15] into Eq. (14). Fig. 7 depicts the sea bottom profile along the line in Fig. 5.

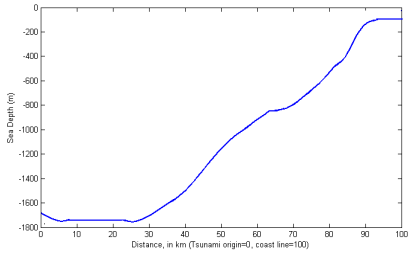

Fig. 7: Sea depth profile at area of interest

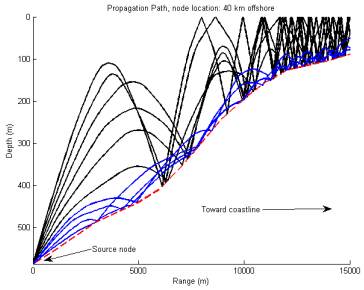

Fig. 8: Propagation path, generated using the Bellhop model

F. Acoustic Propagation Path and Transmission Loss

The varying underwater sound speed, combined with the sea floor profile, determines the propagation path of the acoustic wave. Fig. 8 shows the acoustic wave propagation generated using the Bellhop model, represented in 10 rays in total with departure angle of 10 degrees. The acoustic wave is emitted from a 40 km offshore-source with a frequency of 4 KHz. Due to the variation of undersea sound speed, the acoustic rays follow the paths depicted in Fig. 8. Fig. 9 illustrates the channel loss characteristics when two different acoustic carriers, with frequencies, 4 KHz and 18 KHz, are emitted from two different locations. It can be observed that even when the acoustic waves are transmitted from the same distance, the acoustic waves with different frequencies and locations may produce different channel loss characteristics.

G. Results

1) Minimum Sensor Distance Δ_{min}: Given a set of values of the warning time, Θ_T, listed in table II, the corresponding set of Δ_{min} is determined based on the sea floor profile data, using the equations described in section III-B1 and III-B2. These values represent the initial solutions of the proposed heuristic and are listed in table III.

TABLE III: List of Δ_{min}

Θ_T (minutes)	15	16	17	18	19	20
Δ_{min} (Km)	23.6	25.2	27.1	29.2	31.9	35.5

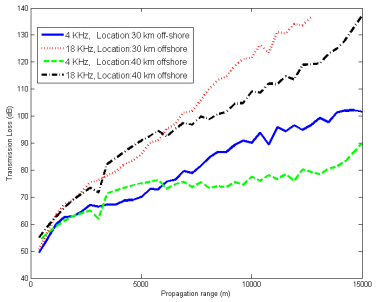

Fig. 9: Channel loss characteristics

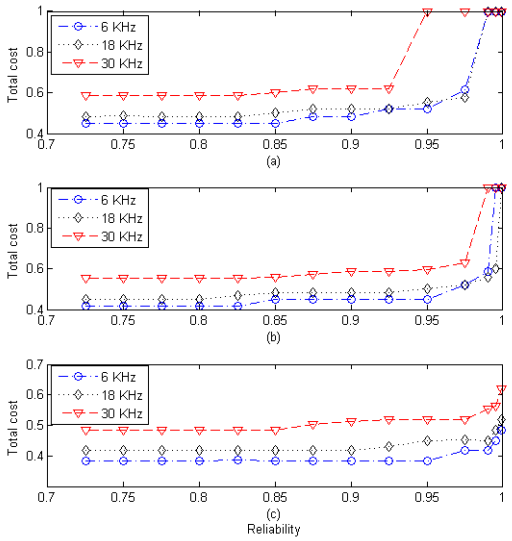

Fig. 10: Total cost for various reliability for 3 different frequencies with $\Theta_T = 20$ minutes

2) The Results under Different Reliability Constraints: The focus is on investigating how the cost optimality can be achieved for different reliability constraints, frequencies and environmental factors. Three different acoustic wave frequencies, 6, 18 and 30 KHz are selected to represent the low, middle and high frequency regions, respectively. In this case, we set Θ_T equals to 20 minutes and maintain the sensor's transmission rate at 120 bps. The remaining constants and parameters used in this experiment are listed in table II. The results are depicted by Fig. 10. The three sub figures, Fig 9(a), 9(b) and 9(c) show the results for severe, moderate and calm environments, respectively.

The results show that the optimal cost of the infrastructure does not increase significantly when the reliability constraint does not exceed 0.925. Consequently, if the desired reliability does not exceed 0.925, a low-cost hybrid infrastructure using a low region of frequencies, is feasible. Achieving higher reliability, however, gives rise to trade-offs between the frequency used and the noise environment.

For example, for a reliability requirement of 0.99, although

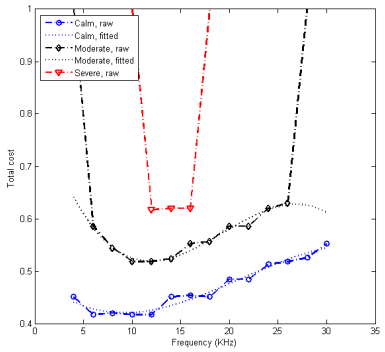

Fig. 11: Total cost for various frequency with $\Theta_R = 0.99$

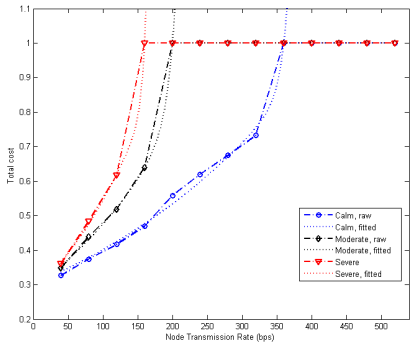

Fig. 12: Total cost for various node transmission rate under 3 different environments, with $\Theta_R = 0.99$

6 KHz frequency results in low-cost infrastructure in a calm environment, using a frequency of 18 KHz achieves minimum cost, C_{tot}, of approximately 2.93% less than the cost of an infrastructure operating with 6 KHz in moderate environment. The difference becomes more notable for higher reliability requirements in severe environment. Rather than using undersea sensors operating with a frequency of 6 KHz, the optimization framework identifies the 18-KHz-based infrastructure a more cost-efficient infrastructure to achieve. The findings provide the basis to determine an optimal carrier frequency for different ambient noise levels. These findings will be discussed in detail in the following section.

3) The Results under Different Carrying Frequencies f: Based on the findings observed in the previous section, a case analysis under different acoustic carrier frequencies and environment factors is the subject of this section. To this end, a reliability constraint of 0.99 is selected while retaining the timeliness constraint at 20 minutes. Fig. 11 shows the results of this study.

The result confirms the findings in section V-G2. Each ambient noise level imposes an optimal frequency range to use in order to achieve the minimum cost. In a calm environment, the optimal cost is achieved for low-range frequencies, namely 6 to 12 KHz. The frequency range shifts to a higher region as the environment becomes noisier.

In moderate environments, the optimal infrastructure cost is achieved for a frequency range of 10 to 16 KHz, whereas in severe environments, the frequencies to achieve optimal cost range from 12 to 18 KHz. Based on these results, an optimal-cost infrastructure to meet the reliability and timeliness constraints in the three different environments can be achieved using a carrier frequency of 12 KHz. For our case study, the minimum cost infrastructure requires 4, 7 and 9 nodes to be deployed for calm, moderate and severe environments, respectively. Table IV lists, for each environment, the distance, d^i, betweeen two consecutive undersea sensors and the length of the optic fiber associated with the configuration.

4) The Results under Different Sensor Tx Rates r_s: This section focuses on investigating the impact to the results due to different undersea node's transmission rates. A frequency of 12 KHz, 20 minutes for the time constraint and 0.99 for the reliability constraint are used. The result is show in Fig. 12.

TABLE IV: Optimal configuration at frequency of 12 KHz

Noise	**Acoustic Link Length (Km)**									L
	d^1	d^2	d^3	d^4	d^5	d^6	d^7	d^8	d^9	**(Km)**
Calm	8.23	8.60	8.85	8.04	-	-	-	-	-	
Moderate	3.08	3.85	4.19	4.10	5.18	4.68	3.49	-	-	10
Severe	1.54	2.50	2.57	3.02	3.09	3.36	3.35	3.13	3.38	11.1

TABLE V: Optimal configuration with node's rate of 40 bps and 160 bps

Node's Rate (bps)	**Number of Sensor N_h (unit)**			**Fiber Optic Length L (Km)**		
	Calm	Moderate	Severe	Calm	Moderate	Severe
40	4	6	7	10	10	10
160	4	7	0	10.27	11.51	35.5

A higher transmission rate requires a shorter acoustic link length to achieve the expected reliability. The cost increases exponentially and becomes more significant in severe noise environments. Table V shows the optimal results for the transmission rates of 40 and 160 bps. A 40 bps transmission rate doesn't incur significant increase in total cost when the environment becomes noisier. The cost increase is contributed by the number of undersea sensors. A more significant cost increase is observed for higher transmission rates. As the noise becomes worse, the cost increase is contributed by both the need of extra underwater sensors and the extension of the fiber optic cable. These results suggest that lower transmission rates is less sensitive to the impact of different ambient noises. However, selecting a very low transmission rate may violate the application data delivery time constraint, especially when larger amount of data are to be sent.

VI. Conclusion and Future Work

The impact of tsunami on humans and the environment can be disastrous, causing severe damage to the infrastructure and great loss of lives, particularly in countries neighboring

the Indian Ocean. Lessons learned from previous tsunamis reveal that a reliable and timely warning system increases the community resilience to tsunami disaster. To this end, we develop an optimization framework, which is used to derive a feasible and cost-effective infrastructure for NFT detection and warning. A case study is used to demonstrate the proposed approach and derive a feasible infrastructure for a region, which is prone to NFT, namely Padang City, West Sumatra, Indonesia. The results show that the proposed approach can lead to the derivation of an infrastructure that can guarantee 20 minute warning time and 99 % data communication reliability.

The proposed framework can be used to provide insights and guidance related to the development and deployment of undersea tsunami detection and warning systems. As future work, the model can further be enhanced by incorporating multi-path loss models for a more realistic communication model and the development of energy management strategies to extend the lifetime of the undersea sensor subnetwork.

ACKNOWLEDGMENT

This material is based in part upon work supported by the National Science Foundation under Grants Number OCE 1331463: Hazards SEES Type 2: From Sensors to Tweeters: A Sustainable Socio-technical Approach for Detecting, Mitigating, and Building Resilience to Hazards. Any opinions, findings, and conclusions or recommendations expressed in this material are those of the authors and do not necessarily reflect the views of the National Science Foundation

REFERENCES

[1] UNESCO-IOC, "Tsunami glossary, 2008," *IOC Technical Series, Paris, France*, vol. 85, 2008.

[2] E. Sasorova, M. Korovin, V. Morozov, and P. Savochkin, "On the Problem of Local Tsunamis and Possibilities of Their Warning," *Oceanology 2008, Pleiades Publishing Inc*, vol. 48, no. 8, pp. 634–645, 2008.

[3] "NDBC- deep-ocean assessment and reporting of tsunamis (DART) description," *[online] http://www.ndbc.noaa.gov/dart/dart.shtml*, visited on April 2014.

[4] L. Comfort, T. Znati, M. Voortman, Xerandy, and L. Freitag, "Early detection of near-field tsunamis using underwater sensor networks." *Science of Tsunami Hazards*, vol. 31, no. 4, 2012.

[5] C. Teng, S. Cucullu, S. M. Arthur, C. Kohler, B. Burnett, and L. Bernard, "Buoy vandalism by noaa national data buoy center," *NOAA National Data Buoy Center1 University of Southern Mississippi2 report*, June 2010.

[6] G. Schmitz, W. Rutzen, and W. Jokat, "Cable-based geophysical measurement and monitoring systems, new possibilities for tsunami early-warnings," in *Underwater Technology and Workshop on Scientific Use of Submarine Cables and Related Technologies, 2007. Symposium on*. IEEE, 2007, pp. 301–304.

[7] M. Porter and Y.-C. Liu, "Finite-element ray tracing," *Theoretical and Computational Acoustics, World Scientific Publishing Co*, vol. 2, 1994.

[8] G. M. Wenz, "Acoustic ambient noise in the ocean: Spectra and sources," *The Journal of the Acoustical Society of America*, vol. 34, no. 12, pp. 1936–1956, 1962. [Online]. Available: http://scitation.aip.org/content/asa/journal/jasa/34/12/10.1121/1.1909155

[9] J. McCloskey, A. Antonioli, A. Piatanesi, K. Sieh, S. Steacy, S. S. Nalbant, M. Cocco, C. Giunchi, J. D. Huang, and P. Dunlop, "Near-field propagation of tsunamis from megathrust earthquakes," *Geophysical Research Letters*, vol. 34, no. 14, 2007. [Online]. Available: http://dx.doi.org/10.1029/2007GL030494

[10] F. B. Jensen, *Computational Ocean Acoustics*. Springer Science & Business Media, 1994.

[11] L. M. Brekhovskikh and I. Lysanov, *Fundamentals of ocean acoustics*.

[12] C. Erbe, *Underwater Acoustics: Noise and the Effects on Marine Mammals, a Pocket Handbook*, 3rd ed. JASCO Applied Sciences, 2011.

[13] M. Porter, "The bellhop manual and userguide: Preliminary draft." [Online]. Available: http://oalib.hlsresearch.com/Rays/HLS-2010-1.pdf

[14] P. C. Etter, *Underwater Acoustics Modeling and Simulation*, 4th ed. CRC Press, 2013.

[15] B. Balai Teknologi Survei Kelautan, "Baruna jaya bppt 2014." [Online]. Available: http://barunajaya.bppt.go.id/index.php/en.html

[16] W.-B. Yang and T. C. Yang, "M-ary frequency shift keying communications over an underwater acoustic channel: Performance comparison of data with models," *The Journal of the Acoustical Society of America*, vol. 120, no. 5, pp. 2694–2701, 2006.

X. Xerandy received the Bachelor and Master degree from Bandung Institute of Technology, Indonesia, majoring in Electrical Engineering in 2006. He joined as the researcher in Agency of Technology Assessment and Application (BPPT), Indonesia since 2008. Currently, he is enrolled as a PhD student in School of Information Science, University Pittsburgh. His primary research is in telecommunication and networking. His current research project is to develop environment-aware undersea sensor network for tsunami disaster mitigation.

Taieb Znati is Professor in the Department of Computer Science, with a joint appointment in Computer Engineering at the School of Engineering. He served as the Director of the Computer and Network Systems Division at the National Science Foundation. He also served as a Senior Program Director for networking research at the National Science Foundation. In this capacity, He led the Information Technology Research Initiative, a cross-directorate research program. Dr. Znatis main research interests are in the design and analysis of evolvable, secure and resilient network architectures and protocols for wired and wireless communication networks. He is also interested in bio-inspired approaches to address complex computing and communications design issues that arise in large-scale heterogeneous wired and wireless networks. He is a recipient of several research grants from government agencies and from industry.

Louise K Comfort is Professor of Public and International Affairs and Director, Center for Disaster Management, University of Pittsburgh. She holds a B.A. in political science and philosophy, Macalester College, a M.A. in political science, University of California, Berkeley, and a Ph.D. in political science, Yale University. She is a Fellow, National Academy of Public Administration, and author or co-author of six books, including Designing Resilience: Preparing for Extreme Events, University of Pittsburgh Press, 2010 and Mega-Crises: Understanding the Prospects, Nature, Characteristics and the Effects of Cataclysmic Events, C. Thomas, 2012. Her primary research interests are in decision making under conditions of uncertainty and rapid change, and the uses of information technology to develop decision support systems for managers operating under urgent conditions.